Planar Three-Dimensional Constrained Lenses

DANIEL T. McGRATH, MEMBER, IEEE

Abstract—**A new design for a beamforming lens is presented. Both faces are planar arrays of radiating elements interconnected by transmission lines whose length varies as a function of radius. While the front face elements are regularly spaced, the back face elements are displaced radially from their corresponding front face elements, the amount of displacement also being a function of radius. We show that such a lens is capable of forming low sidelobe beams over an angular sector 36 beamwidths across in all planes of ϕ by switching between clusters of only seven feed elements. Because both faces are planar, construction of lightweight lenses for multibeam antennas should be feasible.**

I. Introduction

MULTIPLE-BEAM antenna concepts usually call for several feeds sharing a common reflector or lens aperture, with beam steering accomplished by switching between feeds [1]. Because of defocusing effects reflectors (and certain lenses) cannot form low-sidelobe beams over more than a few beamwidths without using large numbers of feed elements, and consequently elaborate beam-switching networks [2], [3]. Multifocal lens antennas have attracted increasing interest because of their superior off-axis focusing, which leads to simpler feeds, and because they lack feed blockage. Yet, those three dimensional lenses developed to date such as metal-plate and dielectric lenses are too heavy and lossy to be practical for large aperture antennas unless they are zoned, which makes them frequency-sensitive and also introduces shadowing effects. Furthermore, they require at least one of the lens surfaces to be curved [4] making fabrication difficult, again, particularly so for large apertures.

This paper introduces a design for a three-dimensional discrete-element, or "constrained" lens whose front and back surfaces are both planar. It uses only two geometric degrees of freedom to achieve good off-axis focusing: the first in the length of transmission line joining elements of opposing faces; and the second in the varying radial position of elements on the back face with respect to those on the front. We will show that such a lens can form low sidelobe pencil beams over a solid angle at least 36 beamwidths across, using clusters of only seven feed elements and no phase or amplitude correction for defocusing.

The general concept is first described in terms of a two-dimensional lens, and later extended to the three-dimensional case. Detailed discussions of its focusing properties and locus of scan are presented. Last, a possible implementation in microstrip is shown as an illustration of the potential ease of fabrication of lightweight lenses for large apertures.

Manuscript received November 15, 1984; revised July 11, 1985.

The author is with the Antennas and RF Components Branch, Electromagnetic Sciences Division, Rome Air Development Center, Hanscom AFB, MA 01731.

IEEE Log Number 8406141.

II. Design Principles, Two-Dimensional Lens

A. The Lens Equations

In contrast to the beamformer designs of Ruze [5] and Rotman [6], we first impose the constraint that both inner and outer lens contours are linear, as shown in Fig. 1. With that limitation, there can be at most two perfect focal points. Since we want a symmetric lens we choose to locate these points at $(y, z) = (-F\cos\theta_0, \pm F\sin\theta_0)$. Path length equality to plane wavefronts directed at, respectively, $\mp\theta_0$ requires

$$[F^2+\rho^2-2\rho F\ \sin\ \theta_0]^{1/2}+W+r\ \sin\ \theta_0=F+W_0 \quad (1)$$

$$[F^2+\rho^2+2\rho F\ \sin\ \theta_0]^{1/2}+W-r\ \sin\ \theta_0=F+W_0 \quad (2)$$

where F is the focal length, W is the electrical line length joining pairs of elements, W_0 is an arbitrary constant and r and ρ are, respectively, the lateral coordinates of elements on the front (aperture side) and back (feed side) faces. Subtracting (2) from (1) and squaring both sides:

$$F^2+\rho^2-2r^2\ \sin^2\ \theta_0=[F^4+\rho^4+2\rho^2F^2-4\rho^2F^2\ \sin^2\ \theta_0]^{1/2}; \quad (3)$$

then squaring both sides again and simplifying leaves

$$\rho=r\left[\frac{F^2-r^2\ \sin^2\ \theta_0}{F^2-r^2}\right]^{1/2} \quad (4)$$

which gives the location of the back face elements in terms of those on the front face. Next we add (1) and (2) to find an expression for the line lengths:

$$W=F+W_0-1/2[F^2+\rho^2-2\rho F\ \sin\ \theta_0]^{1/2} - 1/2[F^2+\rho^2+2\rho F\ \sin\ \theta_0]^{1/2}. \quad (5)$$

B. Path Length Errors and Refocusing

Although we are guaranteed two perfect focal points, we are more interested in how well the lens focuses everywhere else. Assuming for a first approximation that the proper focal arc is a circle of radius F about the center of the lens, then the path length error for a point at angle θ is

$$\frac{\epsilon}{F}=[1+(\rho/F)^2-2(\rho/F)\ \sin\ \theta]^{1/2}+(r/F)\ \sin\ \theta - 1/2[1+(\rho/F)^2-2(\rho/F)\ \sin\ \theta_0]^{1/2} - 1/2[1+(\rho/F)^2+2(\rho/F)\ \sin\ \theta_0]^{1/2}. \quad (6)$$

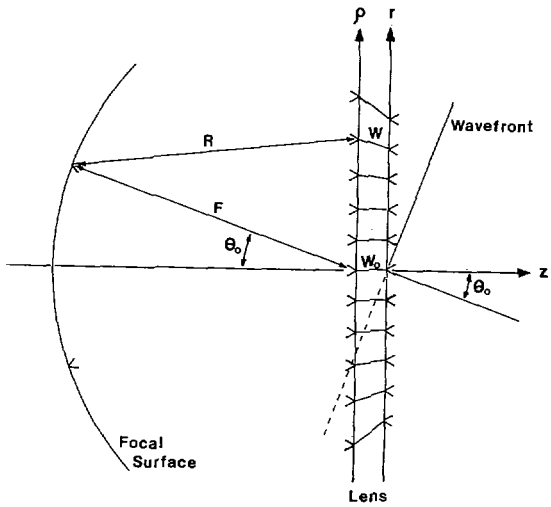

Fig. 1. Linear two degree of freedom (2DF) lens reference geometry.

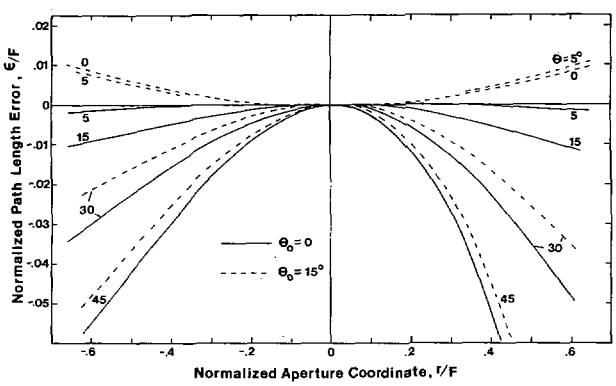

Fig. 2. Path length errors without refocusing. (a) 2DF lens with $\theta_0 = 0$ (solid) and $\theta_0 = 10°$ dashed. (b) Thin lens.

Path length errors are shown in Fig. 2(a) for $\theta_0 = 0°$ and $\theta_0 = 10°$. Fig. 2(b) shows corresponding error contours for a one degree of freedom lens (1DF) which uses line lengths only for focusing:

$$W = F + W_0 - [F^2 + r^2]^{1/2}. \quad (7)$$

Such a lens is the discrete-element analog to an optical "thin lens" since (8) is the same as the "thickness" function for a spherical thin lens [7, p. 80], and is equivalent to the "constant thickness" lens discussed by Ruze [5].

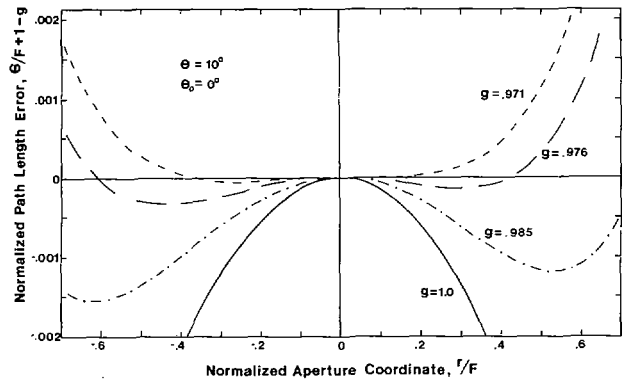

Fig. 3. Path length errors with refocusing for the 2DF linear lens $\theta = 10°$, $\theta_0 = 0$.

Although the magnitude of the errors in Fig. 2(a) are already notably lower than Fig. 2(b), the one degree of freedom errors are mostly cubic functions of r, which are "coma" aberrations [8, p. 212]. In contrast, the two degree of freedom (2DF) errors are mostly second-order "focusing" aberrations which can be reduced by "refocusing," that is moving the feed closer to, or farther away from the lens while maintaining its angle with respect to the lens axis [9].

Fig. 3 shows the resulting path length error when a feed at $\theta = 10°$ is moved closer to the lens, to a distance G, with $g = G/F$. The values $g = 0.976$ and $g = 0.971$ were found (numerically) to minimize the root mean square (rms) error integrated over the aperture for $F/D = 1$ and $F/D = 2$, respectively. The ordinate is $(\epsilon/F + 1 - g)$ since the movement of the feed from F to G introduces a constant path length error of $(G - F)$. This has no effect on the beam quality, and is subtracted to give a clearer representation of the important error terms. It is apparent from the curves $g = 0.971$ and $g = 0.976$ that the peak error is nearly minimized by forcing the error to $(G - F)$ at or near the aperture edge since for $F/D = 1$, $r_{max} = 0.5F$ while for $F/D = 2$, $r_{max} = 0.25F$. Using that condition in (6) we can find an equation for the focal surface. With $\theta_0 = 0$:

$$\epsilon = (G-F) = [G^2 + \rho^2 - 2\rho G \sin\theta]^{1/2} + r \sin\theta - [F^2 + \rho^2]^{1/2}. \quad (8)$$

Substituting $r = F \sin\alpha$; $\rho = F \tan\alpha$

$$(G-F) = [G^2 + F^2 \tan^2\alpha - 2FG \tan\alpha \sin\theta]^{1/2} + F \sin\alpha \sin\theta - F \sec\alpha. \quad (9)$$

Solving for G in (9) leads to

$$g(\theta) = \frac{G}{F} = 1 + \frac{1}{2} \frac{\sin^2\alpha \sin^2\theta}{(1-\sec\alpha)(1+\sin\alpha \sin\theta)}; \quad (10)$$

where $\alpha = \sin^{-1}(r_{max}/F)$. Although (10) is valid only for $\theta_0 = 0$ we have observed a sec θ_0 dependence in numerical computations and thus in general $g(\theta, \theta_0) = \sec\theta_0 g(\theta, 0)$. Fig. 4 shows the shape of the focal arc for a few choices of F/D and θ_0.

Even with refocusing, the path length errors for this lens design are far greater than for an equivalent sized Rotman lens

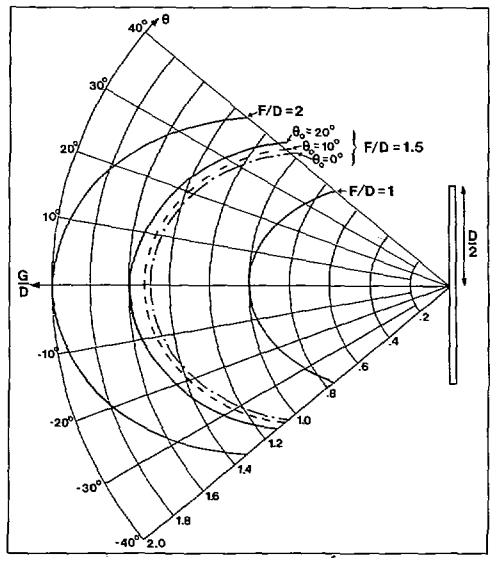

Fig. 4. Optimum focal arc contours for the 2DF linear lens.

[6]. Thus, there is no strong justification for using it as a two-dimensional beamformer. Its chief advantage is in its flat faces, which allows a simpler design of a three-dimensional beamformer for scanning in both azimuth and elevation.

III. Three-Dimensional Lens

A. Extension

No further development is required to extend the design to three dimensions. Equations (4) and (5) still apply but r and ρ are now radial coordinates of front and back face elements as shown in Fig. 5. Instead of a linear array, the front face is a planar array whose lattice geometry is arbitrary. Each front face element at (r_n, ϕ_n) is connected to a back face element at (ρ_n, ϕ_n) by a transmission line of electrical length W_n, with ρ_n and W_n found by applying first (4), then (5).

There are no longer two perfect focal points—θ_0 instead corresponds to a "cone of best focus." As Rao points out [4, p. 1052] designing a three-dimensional lens with more than one perfect focus inevitably destroys its symmetry in ϕ. Since our objective is a lens that focuses well over a large sector in both θ and ϕ, a design with two perfect focal points is undesirable, although we will examine its properties briefly.

B. Errors and Refocusing

In Figs. 6 and 7(a) we show path length error contours for, respectively, a thin lens and a 2DF planar lens, both with their feeds moved 5° off-axis in θ. As in the case of a linear lens, the thin lens has mostly coma error while the 2DF lens has mostly quadratic focus error. Note also that the error contours in Fig. 7(a) are linear, which implies that the beam is perfectly focused in the ϕ plane orthogonal to that containing the feed (ϕ_l is the lens coordinate and ϕ is the feed coordinate). Had we chosen $\theta_0 = \theta = 5°$, the resulting error contours would be identical to Fig. 7(a), except rotated by 90°—the beam would be perfectly focused in its own ϕ plane.

Moving the feed closer to the lens ($G = 0.997F$) reduces the error to that shown in Fig. 7(b). This value of G yields the minimum root mean square (rms) path length error over the aperture. Although the maximum error is reduced considerably, there is no longer any plane in which the beam is perfectly focused. Using a similar analysis to that presented in Section II-B we have found that the focal surface yielding minimum

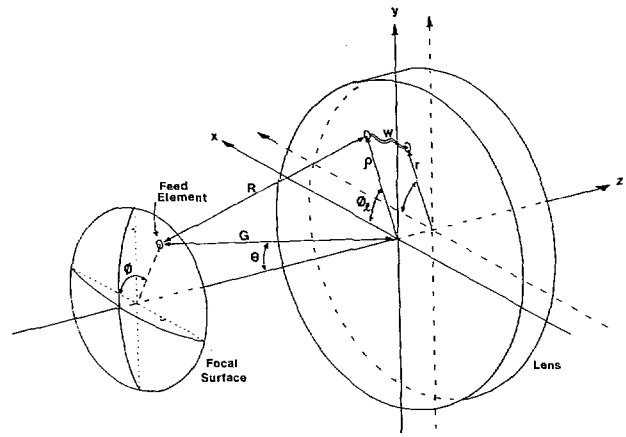

Fig. 5. Planar lens reference geometry.

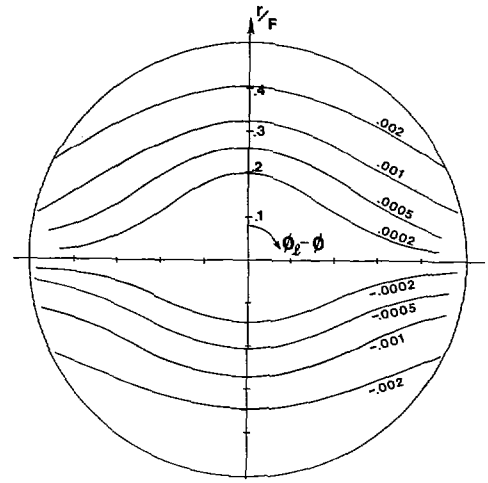

Fig. 6. Path length error contours in the aperture of a thin lens with feed at 5° off-axis.

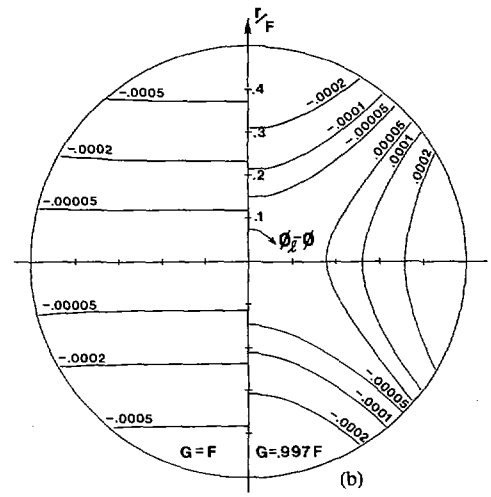

Fig. 7. Path length error contours in the aperture of a 2DF planar lens with feed at 5° off-axis. Left and right sides are, respectively, without and with refocusing.

path length error in any plane of ϕ is, for $\theta_0 = 0$:

$$G(\theta)=F\left[1+1/2 \cdot \frac{\sin^2\alpha \sin^2\theta \cos^2(\phi_l-\phi)}{(1-\sec\alpha)(1+\sin\alpha \sin\theta \cos(\phi_l-\phi))}\right]. \quad (11)$$

Minimizing error in the plane of scan, $\phi_l = \phi$, (11) reduces to (10) and the scan locus is the same as in Fig. 4. However, from Fig. 7 we can conclude that the best contour on which to minimize the error is $\phi_l - \phi = 45°$ and therefore

$$G(\theta)=F\left[1+1/4 \frac{\sin^2\alpha \sin^2\theta}{(1-\sec\alpha)(1+\sin\alpha \sin\theta/\sqrt{2})}\right]. \quad (12)$$

C. Bifocal Planar Lens

In order to derive the design equations for a planar lens with two perfect foci, the path length equality conditions are

$$[F^2+\rho^2\mp 2\rho F \sin\theta_0 \cos\phi_l]^{1/2} + W \pm r \sin\theta_0 \cos\phi_l = F + W_0. \quad (13)$$

Comparing this to (1) and (2) we note that the only difference is that every $\sin\theta_0$ term is now multiplied by $\cos\phi_l$, where ϕ_l is the polar coordinate of a lens element. The term remains intact through the derivation, resulting in the following equations for ρ and W:

$$\rho = r\left[\frac{F^2-r^2 \sin^2\theta_0 \cos^2\phi_l}{F^2-r^2}\right]^{1/2} \quad (14)$$

$$W = F + W_0 - 1/2[F^2+\rho^2-2\rho F \sin\theta_0 \cos\phi_l]^{1/2} - 1/2[F^2+\rho^2+2\rho f \sin\theta_0 \cos\phi_l]^{1/2}. \quad (15)$$

A lens that satisfies (14) and (15) will have two perfect focal points at $(r, \theta, \phi) = (F, \theta_0, 0); (F, \theta_0, 180°)$.

Fig. 8 shows the rms path length error integrated over the lens aperture for several scan planes in ϕ. As expected, the error goes to zero in the principal plane at the angle of perfect focus (10° in this case). Also shown (dashed) is the corresponding error for the ϕ-symmetric lens. It is clear from this figure that a two focal point design only improves the focusing over that part of the scan region within $\sim \pm 35°$ of the principal plane. The poorer focusing elsewhere, particularly near the lens axis is most likely not worth the improvement near the pair of perfect focal points.

D. Pattern Synthesis

Synthesizing low-sidelobe beams with a lens antenna usually requires exciting several feed elements at the same time. White [9] has shown that such beams can only be lossless if the individual patterns of each feed are spatially orthogonal. Assuming that a feed element provides uniform illumination of the aperture it will produce a $J_1(u)/u$ beam (J_1 is the first-order Bessel function) and orthogonality will require that the beam peak coincide with nulls of adjacent beams. Therefore the feeds must be placed at intervals of a beamwidth along the focal arc. For a scanning antenna, it would be convenient to superimpose a triangular array on the focal surface, and scan

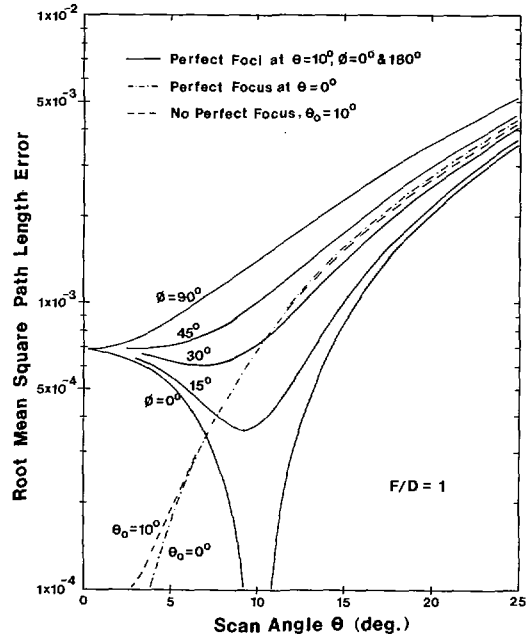

Fig. 8. Root mean square path length errors for 2DF planar lens with two perfect foci (solid) and rotationally symmetric (dashed). All curves include refocusing for minimum rms error.

the beam by switching between clusters of elements. We have found that a seven-element cluster whose six outer elements are weighted 0.3213 relative to the center will (without path length errors) yield peak sidelobes of -36 dB. Fig. 9 shows the pattern of a 100 λ diameter lens with the feed scanned to 12.5° and refocused to $G = 0.982F$ ($F/D = 1$) compared to the on-axis pattern. All sidelobes are well below -30 dB, but the main beam is considerably broader. This spreading is due not only to spherical aberration but also to incomplete aperture illumination: In moving the feed off-axis, we have not adjusted either the amplitude or the phase of its elements ("transverse equalization"). Since opposite edges of the lens are not at the same angle to the off-axis feed's boresight, the aperture taper is slightly skewed. The result is a narrower amplitude distribtion, and a somewhat broader beam.

Based on the results of Fig. 9 we conclude that this lens design is capable of maintaining low sidelobes to at least 18 beamwidths off-axis. Because the lens is symmetric in ϕ, this holds for all scan planes.

IV. Example Design, Microstrip Lens

The fact that both our lens surfaces are planar opens up new possibilities. For illustration only, we consider a lens made up of two microstrip patch arrays facing in opposite directions, with a common ground plane. The aperture side elements are uniformly spaced in a rectangular or triangular lattice, and the corresponding feed side element locations are calculated using (4). The interconnection between elements of opposing faces, as illustrated in Fig. 10, is made with a shorting pin through an aperture in the common ground plane. The two microstrip transmission lines will have a total electrical length of W, given by (5). This should result in an extremely lightweight and inexpensive lens.

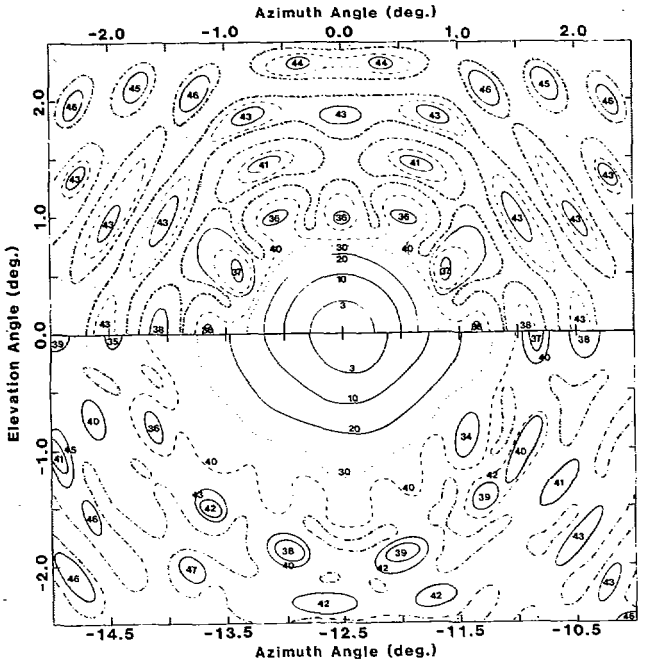

Fig. 9. Calculated antenna patterns for the 2DF planar lens with $F = D = 100\ \lambda$ and $\theta = 0$ using a seven-element feed: (top) on-axis pattern, $G = F$; (bottom) 12.5° scan pattern, $G = 0.982\ F$. Numbering represents relative power in dB below the main beam peak. Shaded areas are below −50 dB.

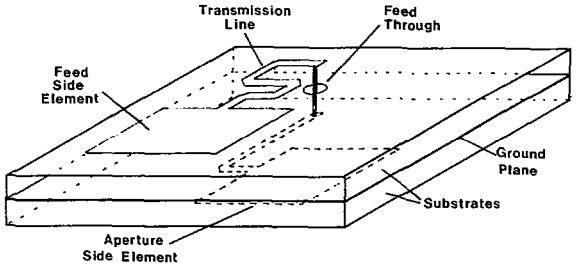

Fig. 10. Element design and interconnection for a microstrip constrained lens.

V. Conclusion

The design of a three-dimensional bootlace lens with planar front and back faces has been presented. Using two degrees of freedom, line lengths and radial displacement of back face elements, its off-axis focusing properties are sufficient to allow scanning of a 0.7° low sidelobe beam over at least a 25° solid angle. Because this lens does not require correction for scanning aberrations, the focal array and its feed network can be relatively simple compared to array feeds for reflector antennas. The comparison to a bifocal lens indicates that a lens does not necessarily need any perfect focal points to scan over wide angles. The most important feature of the two degree of freedom design, however, is the potential ease of fabrication.

References

[1] L. J. Ricardi, "Communication satellite antennas," *Proc. IEEE,* vol. 65, pp. 356–369, Mar. 1977.

[2] A. W. Rudge and M. J. Withers, "New technique for beam steering with fixed parabolic reflectors," *Proc. Inst. Elec. Eng.*, vol. 118, pp. 857–863, July 1971.

[3] A. V. Mrstik, "Effects of phase and amplitude quantization errors on hybrid phased-array reflector antennas," *IEEE Trans. Antennas Propagat.*, vol. AP-30, pp. 1233–1236, Nov. 1982.

[4] J. B. L. Rao, "Multifocal three-dimensional bootlace lenses," *IEEE Trans. Antennas Propagat.*, vol. AP-30, pp. 1050–1056, Nov. 1982.

[5] J. Ruze, "Wide-angle metal-plate optics," *Proc. IRE,* vol. 38, pp. 53–59, Jan. 1950.

[6] W. Rotman and R. F. Turner, "Wide-angle microwave lens for line source applications," *IEEE Trans. Antennas Propagat.*, vol. AP-11, pp. 623–632, Nov. 1963.

[7] J. W. Goodman, *Introduction to Fourier Optics.* New York: McGraw-Hill, 1968.

[8] M. Born and E. Wolf, *Principles of Optics.* New York: MacMillan, 1964.

[9] W. D. White, "Pattern limitations in multiple-beam antennas," *IRE Trans. Antennas Propagat.*, vol. AP-18, pp. 430–436, July 1962.

Daniel T. McGrath (S'82–M'82) was born in Tampa, FL, in 1956. He received the B.S.E.E. degree from the United States Air Force Academy, Colorado Springs, CO, in 1979 and the M.S.E.E. degree from the Air Force Institute of Technology, Dayton, OH, in 1982.

From 1979 to 1981 he worked in the Munitions Division of the Air Force Armament Laboratory, Eglin AFB, FL. Since January 1983 he has been with the Rome Air Development Center's Electromagnetic Sciences Division, Hanscom AFB, MA. Current research includes the development of lens antennas and related concepts.

Capt. McGrath is a member of the IEEE Antennas and Propagation and Acoustics, Speech and Signal Processing Societies, and of Tau Beta Pi and Eta Kappa Nu.